



Titre: Three-mode photonic lanterns: comprehensive analysis from theory to experiments. Supplément
Title:

Auteurs: Rodrigo Itzamná Becerra-Deana, Raphaël Maltais-Tariant, Guillaume Ramadier, Martin Poinset De Sivry-Houle, Stéphane Virally, Caroline Boudoux, & Nicolas Godbout
Authors:

Date: 2025

Type: Article de revue / Article

Référence: Itzamná Becerra-Deana, R., Maltais-Tariant, R., Ramadier, G., Poinset De Sivry-Houle, M., Virally, S., Boudoux, C., & Godbout, N. (2025). Three-mode photonic lanterns: comprehensive analysis from theory to experiments. Optics Continuum, 4(6), 1198-1211. <https://doi.org/10.1364/optcon.564008>
Citation:

 **Document en libre accès dans PolyPublie**
Open Access document in PolyPublie

URL de PolyPublie: <https://publications.polymtl.ca/65582/>
PolyPublie URL:

Version: Matériel supplémentaire / Supplementary material
Révisé par les pairs / Refereed

Conditions d'utilisation:
Terms of Use:

 **Document publié chez l'éditeur officiel**
Document issued by the official publisher

Titre de la revue: Optics Continuum (vol. 4, no. 6)
Journal Title:

Maison d'édition: Optica Publishing Group
Publisher:

URL officiel: <https://doi.org/10.1364/optcon.564008>
Official URL:

Mention légale:
Legal notice:

Three-mode photonic lanterns: comprehensive analysis from theory to experiments: supplement

RODRIGO ITZAMNÁ BECERRA-DEANA,^{1,2}  RAPHAEL MALTAIS-TARIANT,^{1,3}  GUILLAUME RAMADIER,¹ MARTIN POINSINET DE SIVRY-HOULE,¹  STÉPHANE VIRALLY,¹  CAROLINE BOUDOUX,^{1,2,3}  AND NICOLAS GODBOUT^{1,2,*} 

¹*Polytechnique Montréal, 2500 Chemin de Polytechnique, Montréal, QC H3T 1J4, Canada*

²*Castor Optics, 361 Boulevard Montpellier, Saint-Laurent, QC H4N 2G6, Canada*

³*CHU Sainte-Justine, 3175 Chemin de la Côte Sainte-Catherine, Montréal, QC H3T 1C5, Canada*

**nicolas.godbout@polymtl.ca*

This supplement published with Optica Publishing Group on 4 June 2025 by The Authors under the terms of the [Creative Commons Attribution 4.0 License](https://creativecommons.org/licenses/by/4.0/) in the format provided by the authors and unedited. Further distribution of this work must maintain attribution to the author(s) and the published article's title, journal citation, and DOI.

Supplement DOI: <https://doi.org/10.6084/m9.figshare.28950638>

Parent Article DOI: <https://doi.org/10.1364/OPTCON.564008>

Three-Mode Photonic Lanterns: Comprehensive Analysis from Theory to Experiments - Supplemental Document

1. ADIABATIC CRITERIA AND LOGARITHMIC SLOPE

In the context of fiber devices, adiabaticity refers to the absence of coupling of one specific mode with any other mode. This happens as long as the logarithmic slope $\frac{1}{I} \frac{\partial I}{\partial z}$ remains below the adiabatic criteria $\bar{\alpha}_{ij}$ between the specific mode i and all other modes j , at every point along the taper

$$\frac{1}{I(z)} \frac{\partial I(z)}{\partial z} < \min_j \bar{\alpha}_{ij}(z) \quad \forall z. \quad (\text{S1})$$

If an adiabatic criterion becomes lower than the logarithmic slope for a significant amount of time, amplitude interference between modes will occur, and power will potentially be transferred from one mode to another. Tools such as SuPyMode compute adiabatic criteria for custom structures at various inverse taper ratios (ITRs). They can, in turn, be compared to the logarithmic slope expected from the fabrication sequence [1].

The computation of the logarithmic slope is described in reference [2], where a longitudinal section of length

$$L = L_0 + \alpha \delta z \quad (\text{S2})$$

is heated up. Here, L_0 is the initial length of the heated section, α is a unitless coefficient (see below), and δz is the total elongation of the component (i.e., the difference between the current length of the component and its initial length). The coefficient α ranges from -1 to $+1$: a positive value indicates an increase in the length of the heated segment as the fabrication progresses. A negative value means a decrease of that same length throughout the recipe. The value of α determines the longitudinal shape of the component, following

$$I(z) = \left[1 + \frac{2\alpha z}{L_0(1-\alpha)} \right]^{-\frac{1}{2\alpha}}, \quad (\text{S3})$$

such that the choice of fabrication parameters L_0 and α is sufficient to determine the logarithmic slope along the component and, thus, the expected adiabaticity of the component. In general, smaller values of L_0 and α yield shorter components, which is beneficial for robustness at the cost of increasing the logarithmic slope and, thus, the potential of coupling between modes.

For a photonic lantern (PL) with a final few-mode structure of $\sim 10 \mu\text{m}$ of diameter, L_0 is limited to the range between the size of the heating element (typically around 1 mm) and the length at which the component becomes too fragile for practical purposes (typically 10 mm).

Furthermore, heuristics dictate that the manufacturability of fused components is limited to adiabatic criteria greater than 10^{-4} .

Fig. S1 presents the design of a three-mode mode-selective photonic lantern (MSPL) using single-mode fibers. The simulation was performed using SuPyMode [1, 3]. Fig. S1 (a) shows the cross-section of the fiber bundle making up the 3-mode MSPL after an initial fusion with a degree of fusion of 0.8—the degree of fusion varying between 0 (no fusion) and 1 (fully-fused structure). The core diameters of the single-mode fibers are 8, 10, and 12 μm for fibers labeled A', B', and C', respectively, with refractive indices equivalent to those of the typical SMF-28 (ITU-T 6.657.A1, Corning, NY, USA) for the core and cladding in all cases. Fig. S1 (b, top row) shows the field amplitudes of the transverse modes at the single-mode inputs. Fig. S1 (b, bottom row) shows the corresponding outputs for an ITR=0.05, i.e., at the end of the tapering process. Note that the scale changes between the top and bottom row of Fig. S1 (b). At the top, the full-scale is the structure before tapering, while the scale at the bottom is that of the minimum cross-section

(waist) after tapering. The first three columns show the three desired modes obtained from selective LP₀₁ illumination. The last three columns show that other higher-order modes (e.g., LP₂₁ and LP₀₂) can be obtained by illuminating with non-fundamental modes (LP₁₁). In reality, this cannot happen as those modes are unguided in the structure. Instead, coupling to those modes creates loss channels and contributes to excess loss. For the structure simulated in Fig. S1, the only guided modes of interest are the fundamental mode LP₀₁ and the first two higher order modes, LP_{11_a} and LP_{11_b}.

Fig. S1 (c) displays adiabatic criteria computed by coupled-mode theory (CMT) (in solid lines) and the logarithmic slopes (dashed lines) as a function of ITRs, computed for different values of α . In this example, three different taper fabrication recipes are depicted, represented by a null, a positive, and a negative α , respectively, each with an initial value of $L_0 = 10$ mm.

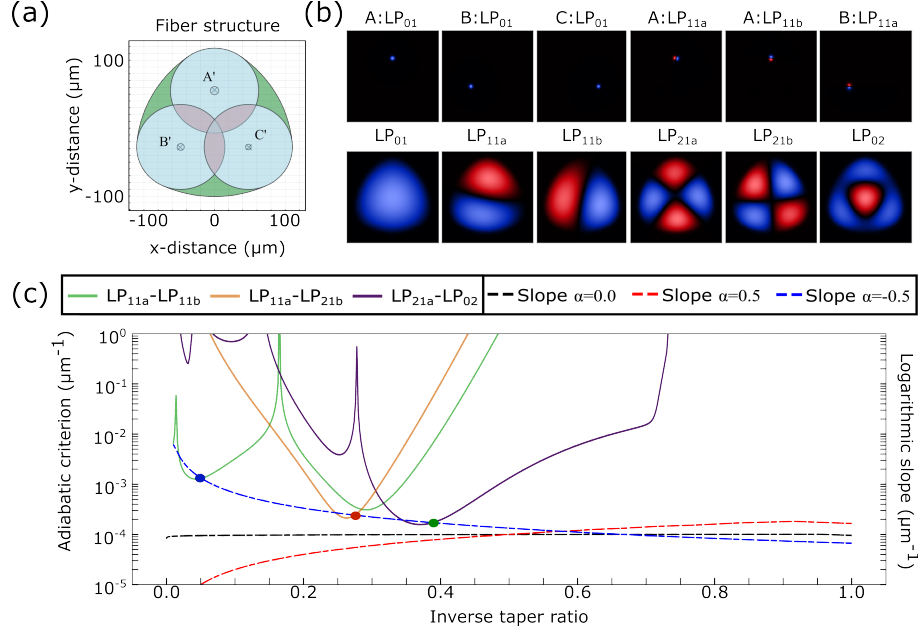


Fig. S1. Simulating the design of a 3-mode MSPL with single-mode fibers. (a) Cross-section of the MSPL after fusion using a fusion coefficient of 0.8. (b) Field amplitudes of the transverse modes at the input (first row) and after tapering (ITR=0.05—second row). (c) Adiabatic criteria for each mode pair (solid lines) and logarithmic slopes (dashed lines) for three fabrication sequences using an initial heating length of 10 mm and three different α values. The red and blue dots show instances of crossing between α and mode mode-coupling curves.

For practical purposes, only the three most relevant curves are plotted into Fig. S1(c) to highlight the possible responses of the device. In contrast, Fig. S2 presents the typical “jungle” of adiabatic criteria produced by the model. Ideally, all modes that interact with the guided modes should be included in the plot. However, adiabatic criteria between higher-order modes tend to be larger, and a cutoff of about 20 pairs is usually implemented in the code to avoid computing too many irrelevant criteria.

Three main crossing types are shown in Fig. S1(c). They all occur with the blue dashed line, which represents the design with the steepest slopes. The blue dot corresponds to a crossing between two guided modes, leading to power transferred between the modes. This is intended in some components, such as conventional PLs or standard couplers. The red dot illustrates a crossing between a guided and an unguided modes. These are always to be avoided, as they result in excess loss. The green dot indicates coupling between two unguided modes, which does not affect the structure at all as these modes do not propagate. In components such as MSPLs, all types of crossings are avoided, leading to full modal isolation.

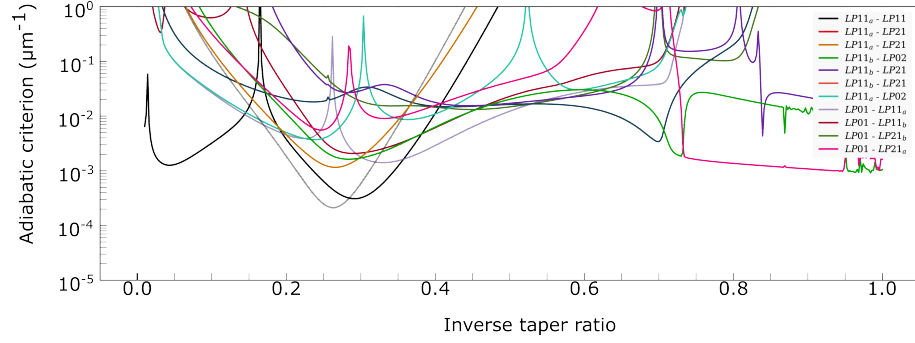


Fig. S2. Adiabatic criteria for each mode pair of a 3-mode MSPL with single-mode fibers.

2. FURTHER ANALYSES

To fabricate any component, it is crucial to run simulations at various wavelengths and with different fusion degrees. This is important in particular when the exact degree of fusion cannot be determined in advance, and when the component is intended to be broadband.

Figure S3 shows four distinct columns. The first column represents the degree of fusion for a 3-by-1 structure of each row with the fiber configuration ABC, as described in the paper. The second, third, and fourth columns illustrate the adiabatic criteria for the first four pairs of modes at three wavelengths: 1550 nm, 1300 nm, and 1100 nm. This example illustrates an MSPL, which is the most stable structure. It is intended as a didactical shortcut by simplifying the analysis while still identifying changes in behavior that can arise during the fabrication process. We observe, for instance, that the adiabatic criteria tend to increase with the degree of fusion. Interestingly, at reduced degrees of fusion, coupling starts to occur at smaller ITRs. Finally, as wavelength increases, the areas of potential coupling tend to compactify. It is thus expected that for the same recipe, relatively less coupling will occur at higher wavelengths.

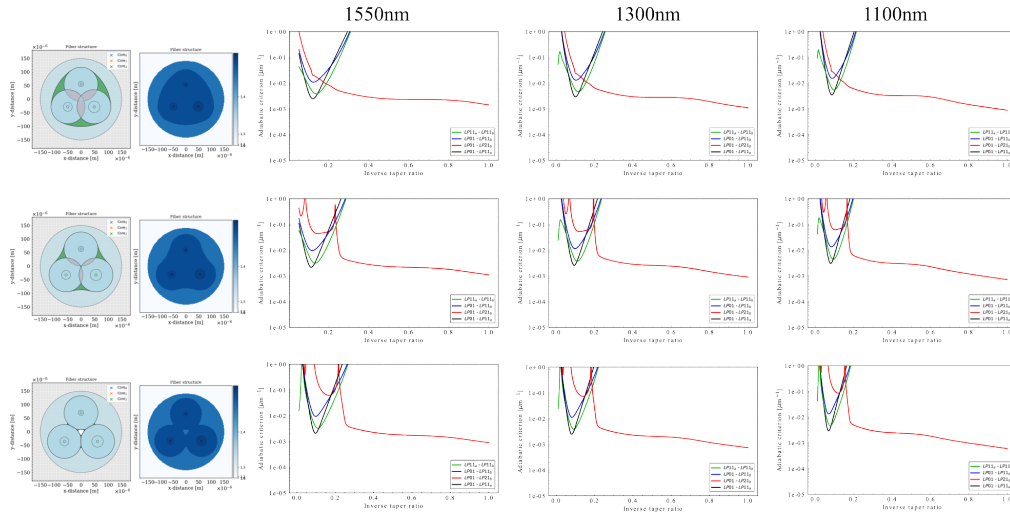


Fig. S3. Analysis of the adiabatic criteria at different degrees of fusion and wavelengths. The first column details the degree of fusion corresponding to each row, using the ABC fiber configuration described in the paper. The second, third, and fourth columns display the adiabatic criteria for the first four pairs of modes across three wavelengths: 1550 nm, 1300 nm, and 1100 nm.

Figure S4 shows the adiabatic criteria for the first four pairs of modes at three different wavelengths (merging the plots of the three degrees of fusion).

In contrast, Figure S5 shows the adiabatic criterion at three distinct degrees of fusion while combining the plots for the three wavelengths.

Figure S6 shows the adiabatic criteria for all degrees of fusion and all wavelengths. This

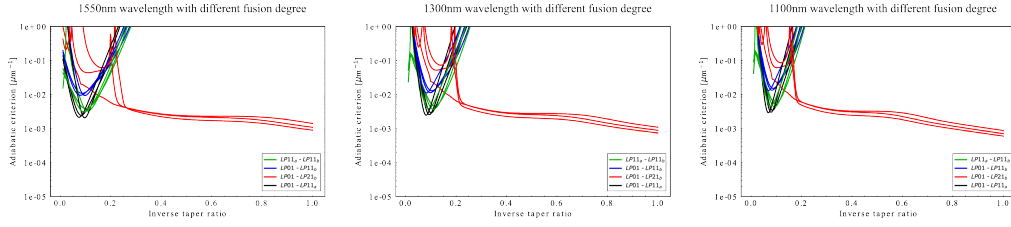


Fig. S4. Adiabatic criteria of an MSPL at 1550 nm, 1300 nm, and 1100 nm for the initial four pairs of modes used in combining all the fusion degrees.

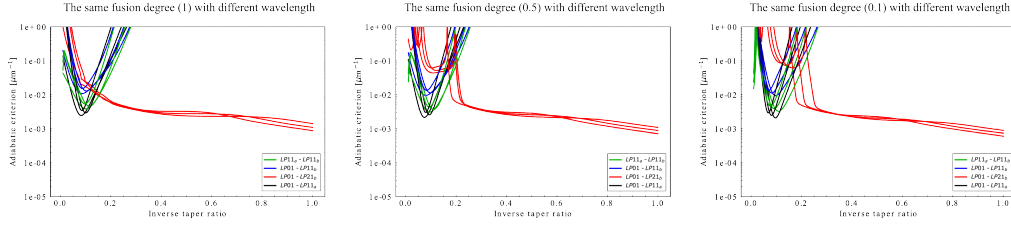


Fig. S5. Adiabatic criteria for the initial four pairs of modes of an MSPL at three different fusion degrees, combining the three operational wavelengths: 1550 nm, 1300 nm, and 1100 nm

enables to consolidate our view of all potential variations of behavior during fabrication. A good fabrication sequence for an MSPL would steer the logarithmic slope away from all the adiabatic criteria curves in this plot.

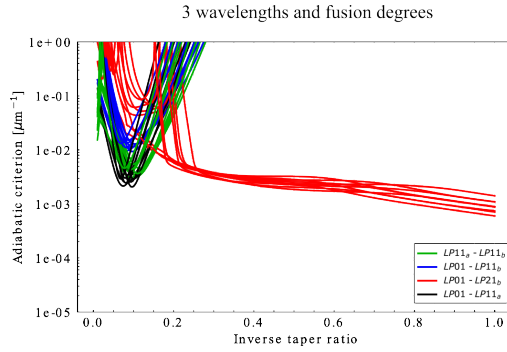


Fig. S6. Adiabatic criteria for each mode pair of a 3-mode MSPL at three fusion degrees and wavelengths.

REFERENCES

1. M. Poinset de Sivry-Houle, R. I. Becerra-Deana, S. Virally, *et al.*, "Supymode: an open-source library for design and optimization of fiber optic components," *Opt. Continuum* **3**, 242–255 (2024).
2. T. Birks and Y. Li, "The shape of fiber tapers," *J. Light. Technol.* **10**, 432–438 (1992).
3. M. Poinset de Sivry-Houle, "Martinpdes/supymode: 1.0.0," (2023).